JEE Journal of Ecological Engineering

Journal of Ecological Engineering, 2026, 27(11), 253–272
https://doi.org/10.12911/22998993/226072
ISSN 2299–8993, License CC-BY 4.0

Received: 2026.06.05
Accepted: 2026.09.15
Published: 2026.10.01

Research on the electromechanical system of an autonomous photovoltaic station for hybrid power supply of pumping equipment and lighting of livestock complexes

Oleksandr Vozniak[1], Andrii Shtuts[1], Ihor Kupchuk[1], Inna Teliatnyk[1*]

[1] Vinnytsia National Agrarian University, 3 Sonyachna Street, 21008 Vinnytsia, Ukraine
* Corresponding author's e-mail: inna201098@gmail.com

ABSTRACT

The article investigates the electromechanical system of an autonomous photovoltaic station designed for hybrid power supply of pumping equipment and lighting in livestock complexes. The relevance is determined by the need to improve the reliability, energy efficiency, environmental sustainability, and autonomy of power supply to agricultural facilities under unstable operation of centralized power grids, rising energy costs and renewable energy technologies. The system integrates a photovoltaic array, an MPPT controller, a PWM inverter, a three-phase induction motor driving a pumping unit, an energy-storage unit, and an LED lighting subsystem. The selection of the AXM144-9-166-470 photovoltaic panel with a rated power of 470 W and a 7.5 kW induction motor was substantiated. A single-diode photovoltaic-module model was applied, taking into account solar irradiance, temperature, and series and parallel resistances. The research methodology combined mathematical modeling and simulation in MATLAB/Simulink R2023b, experimental assessment of illumination in livestock premises, and a simplified comparative life-cycle greenhouse-gas assessment of photovoltaic and diesel-based power-supply scenarios. The transient processes of the pumping unit were investigated at DC-link voltages of 490 and 390 V. At 490 V, the system ensured stable start-up, and the motor reached the specified speed within approximately 1.1 s. Reducing the input voltage to 390 V decreased the motor voltage, currents, electromagnetic torque, and power consumption; however, the system remained dynamically stable and reached a new steady state without emergency shutdown. The lighting subsystem was evaluated using luxmeter measurements, experimentally determined luminous-intensity curves, and nonlinear regression. A 70 W ZhKU-11U-70-011 sodium luminaire and a 45 W LED luminaire were compared. The LED luminaire reduced installed lighting power by 35%, whereas the sodium luminaire provided a greater effective lighting range because of its light-distribution characteristics. For a functional unit of 66 kWh/day, the simplified assessment indicated approximately 52.47 kg CO_2-eq./day for diesel generation and 3.04 kg CO_2-eq./day for photovoltaic electricity, corresponding to a reduction of about 94.2%. Over 25 years, the estimated greenhouse-gas impact of the photovoltaic scenario was approximately 17 times lower. The results confirm the feasibility of combining MPPT control, scalar U/f regulation, energy storage, and energy-efficient LED lighting to improve the technical and environmental performance of autonomous power-supply systems for livestock complexes.

Keywords: pumping station, lighting, renewable energy, energy storage, electromechanical system, hybrid power supply, livestock complex, autonomous water supply.

INTRODUCTION

One of the most important needs of humanity is water. Most human activities rely on free access to adequate water resources to ensure food production, domestic needs, health care, electricity generation and ecosystem restoration (Stadnik et al., 2025a; Abbasi and Mohammadi, 2024). All societies need water for sustainable social and economic development, and ensuring a stable water supply is one of the key priorities at both the global and regional levels (Koval et al., 2025a). Water supply throughout history has remained a pressing technical challenge, especially acute in poor, arid and rural regions where the infrastructure of centralized electricity supply is underdeveloped or absent (Kumar and Sahu, 2022; Kumar and Singh, 2018).

Livestock complexes are among the most energy-intensive objects of agricultural production (Stadnik et al., 2025a; Hontaruk et al., 2026). They require continuous electricity supply to ensure two critically important functions: water supply for livestock and lighting for production facilities (Stadnik et al., 2025a). The quality and continuity of water supply directly affects animal productivity, the sanitary condition of the farm and the overall efficiency of the production process (Hontaruk et al., 2026). In turn, proper lighting of production premises is a necessary condition not only for the work of personnel, but also for compliance with zootechnical standards that regulate the length of daylight hours for various species of farm animals and poultry (Stadnik et al., 2025a; Hontaruk et al., 2026). Thus, interruptions in the power supply of livestock complexes can lead to significant economic losses and deterioration of animal housing conditions (Stadnik et al., 2025a; Aliiev et al., 2026; Augustyn et al., 2021).

For irrigation of crops, pumping water for domestic needs and watering livestock, pumping systems with an appropriate power source are required (Stadnik et al., 2025c; Koval et al., 2025a). In rural areas, energy sources may be located at a considerable distance from water sources, and the installation of new power lines and transformers in isolated locations is extremely expensive and technically complex (Kumar and Sahu, 2022; Abbasi and Mohammadi, 2024). Unstable quality of electricity in rural distribution networks, frequent outages and significant voltage deviations further exacerbate the problem of reliable power supply to agro-industrial facilities (Stadnik et al., 2025c).

Existing systems based on internal combustion motors used for autonomous pumped water supply and backup power supply have significant disadvantages: the need for regular maintenance and refueling, high cost of fuel, dependence on the logistics of its supply, significant noise during operation and negative impact on the environment due to emissions of combustion products (Hontaruk et al., 2026; Abbasi and Mohammadi, 2024). In the context of rising energy prices and increasing environmental requirements, these disadvantages are becoming an increasingly compelling argument in favor of finding alternative solutions (Koval et al., 2025a). That is why the use of renewable energy is particularly attractive for autonomous water pumping and lighting systems in rural areas (Stadnik et al., 2025a; Errouha et al., 2020; Burlaka et al., 2024).

Generating electricity using photovoltaic cells is one of the most promising renewable sources for the needs of livestock complexes (Stadnik et al., 2025a; Koval et al., 2025a). The advantages of photovoltaic systems are: relative ease of installation, low infrastructure requirements, stability and noiselessness of operation due to the absence of rotating machines and turbines, the possibility of application directly at the place of use, long service life and low regular maintenance (Errouha et al., 2020; Kumar and Singh, 2018).

The use of autonomous photovoltaic systems should contribute to improving economic conditions in remote areas, increasing the energy independence of agricultural enterprises and preserving the environment (Hontaruk et al., 2026; Abbasi and Mohammadi, 2024). The key component of such a system is the electromechanical subsystem, which ensures interaction between the photovoltaic energy source and consumers – the pumping unit and the lighting system (Hontaruk et al., 2024; Patel and Shah, 2025). The efficiency, stability and reliability of the entire hybrid power supply complex directly depend on the correct design and configuration of this subsystem (Stadnik et al., 2025a; Patel and Shah, 2025). An important role is played by the choice of the type of electric drive, the control algorithm and the method of selecting the maximum power from the photovoltaic panels – MPPT – depending on the current weather conditions and the level of insolation (Hontaruk et al., 2024; Errouha et al., 2021).

Global energy demand continues to increase, while dependence on finite fossil-fuel resources and the environmental consequences of their combustion strengthen the need for renewable electricity generation. For agricultural facilities located in rural areas, distributed photovoltaic generation is particularly relevant because it can reduce dependence on long distribution lines and fuel-delivery logistics (Errouha et al., 2020; Kumar and Singh, 2018; Abbasi and Mohammadi, 2024).

For livestock facilities, the principal research challenge is not merely the availability of a renewable source but the coordinated operation of variable photovoltaic generation, energy storage, a motor-driven pumping load, and lighting. Reliable control is therefore required to maintain water supply and acceptable lighting conditions when solar irradiance changes (Hontaruk et al., 2024; Patel and Shah, 2025).

The traditional backup solution for such facilities is diesel generators, but they have significant limitations: high cost and instability of fuel prices, the need for regular maintenance, significant noise levels and harmful emissions into the atmosphere (Stadnik et al., 2025a; Abbasi and Mohammadi, 2024). In the context of increasing energy costs and tightening environmental legislation, such solutions are becoming less and less acceptable from an economic and environmental point of view (Koval et al., 2025a; Hontaruk et al., 2026). An alternative is the creation of hybrid power supply systems based on photovoltaic plants, which are able to provide autonomous and reliable power supply to livestock complexes – both pumping equipment for water supply and lighting systems (Stadnik et al., 2025a; Hontaruk et al., 2026).

However, the implementation of such systems is associated with a number of technical problems. First, the output power of photovoltaic panels significantly depends on weather conditions – the level of insolation and temperature, which causes instability of voltage in the system (Errouha et al., 2020; Kumar and Singh, 2018). Secondly, coordinating the operation of the photovoltaic source with the asynchronous electric drive of the pumping station requires the use of specialized control algorithms, in particular MPPT and frequency control (Hontaruk et al., 2024; Kumar and Sahu, 2022). Thirdly, the simultaneous power supply of two dissimilar loads – the pumping unit and the lighting system – requires the development of an effective system for distributing and prioritizing electricity (Stadnik et al., 2025a).

Solving these problems by studying and optimizing the electromechanical system of an autonomous photovoltaic station is an urgent scientific and technical task that has direct practical significance for increasing energy independence and efficiency of livestock complexes (Stadnik et al., 2025a; Patel and Shah, 2025).

An effective means of ensuring reliable and high-quality power supply to responsible consumers is the development and implementation of autonomous (uninterruptible) power supply systems (UPS), which contain several sources of electricity - main, backup and emergency (Stadnik et al., 2025a; Selem et al., 2023). Livestock complexes belong to the category of responsible consumers, since interruptions in their power supply cause direct economic losses and negatively affect the condition of animals (Stadnik et al., 2025a; Hontaruk et al., 2026). The limited resources of organic fuel and the negative environmental consequences of traditional energy open up broad prospects for the use of renewable energy sources (RES), primarily photovoltaic and wind installations, as part of the UPS (Kumar and Singh, 2018; Koval et al., 2025a). One of such autonomous systems is a photovoltaic power supply system.

It consists of interconnected components designed to ensure efficient delivery of electrical energy from the source of generation to the load (Stadnik et al., 2025a; Koval et al., 2025a). Depending on the configuration and application conditions, such systems can power both individual devices and extensive load networks that include heterogeneous consumers - pumping equipment and lighting systems (Stadnik et al., 2025a; Hontaruk et al., 2026). Photovoltaic power supply systems are classified into three main categories: grid-connected, stand-alone and hybrid (Errouha et al., 2020; Kumar and Singh, 2018). Grid-connected systems transfer excess generated electricity to the general power system and can receive energy from it in case of insufficient generation (Abbasi and Mohammadi, 2024). Stand-alone systems operate completely independently of the centralized network and provide power to consumers exclusively from their own generation and accumulated reserves (Kumar and Sahu, 2022; Kumar and Singh, 2018). Hybrid systems combine several energy sources - photovoltaic panels, diesel generators, wind turbines - and are the most flexible solution for complex operating conditions (Stadnik et al., 2025a; Hontaruk et al., 2026).

In grid-connected and stand-alone systems, energy storage elements – batteries or supercapacitors – can be used to accumulate excess energy and use it at night or during periods of insufficient solar radiation (Errouha et al., 2021; Koval et al., 2025a). For livestock complexes that require 24-hour power supply, the presence of an energy storage system is a prerequisite for the reliable operation of an autonomous photovoltaic plant (Stadnik et al., 2025a; Hontaruk et al., 2026).

In stand-alone systems, the power of photovoltaic panels is directly supplied to the load without connection to the utility grid (Kumar and Sahu, 2022; Koval et al., 2025a). Such systems are considered one of the most economically feasible ways to implement photovoltaic generation, especially for facilities in rural areas with intense solar radiation and limited or unreliable access to centralized networks (Stadnik et al., 2025a; Abbasi and Mohammadi, 2024). Typical examples of applications are water supply and watering systems for livestock, lighting for livestock facilities, communication systems, beacons, emergency services and military facilities (Stadnik et al., 2025a; Hontaruk et al., 2026).

At the same time, stand-alone systems have certain disadvantages and limitations that must be taken into account when designing (Errouha et al., 2020; Koval et al., 2025a). First, since the system is not connected to the utility grid, the presence of a storage element is mandatory, which leads to additional capital costs for batteries and charge controllers (Errouha et al., 2021; Koval et al., 2025a). In the absence of a storage element, the excess generated power is dissipated and lost (Errouha et al., 2021). Secondly, in autonomous systems, the operating power must correspond to the maximum load demand, which requires careful calculation and selection of equipment at the design stage (Errouha et al., 2020; Kumar and Singh, 2018). Thirdly, batteries have a limited resource of charge-discharge cycles and require regular maintenance and timely replacement (Koval et al., 2025a; Abbasi and Mohammadi, 2024).

To overcome these limitations in the power supply systems of livestock complexes, it is promising to use a hybrid approach that combines photovoltaic generation with a backup power source and an intelligent load distribution control system between pumping equipment and lighting (Stadnik et al., 2025a). The MPPT algorithm improves energy extraction from photovoltaic panels under varying irradiance and temperature conditions (Hontaruk et al., 2024; Errouha et al., 2021), and the use of frequency control of the asynchronous electric drive of the pumping station provides an optimal ratio between the generated power and the current needs of the water supply system (Kumar and Sahu, 2022; Patel and Shah, 2025). Such a comprehensive approach to the organization of power supply of livestock complexes allows to significantly increase the reliability, economy and environmental friendliness of their power supply (Stadnik et al., 2025a; Hontaruk et al., 2026).

The purpose of this work is to increase the efficiency and environmental sustainability of power supply for livestock complexes by developing and substantiating the operating processes of an electromechanical system based on an autonomous photovoltaic station. To achieve this purpose, the system structure and principal components were analyzed; the main equipment was selected and substantiated; a mathematical model was developed in MATLAB/Simulink; transient processes were investigated at nominal and reduced DC-link voltages; the lighting subsystem was evaluated experimentally; and a simplified comparative assessment of greenhouse-gas emissions, life-cycle impacts, circular-economy criteria, and contributions to the UN Sustainable Development Goals was performed.

RESEARCH METHODOLOGY

Composition and technical parameters of the studied electromechanical system

The studied hybrid power supply system of the livestock complex consists of the following interconnected components: an array of solar photovoltaic (PV) panels, a maximum power point tracking (MPPT) controller, a PWM inverter on IGBT transistors, an asynchronous electric drive of the pumping station, an energy storage unit, and a lighting power supply subsystem.

The main energy source is a monocrystalline silicon photovoltaic panel AXM144-9-166-470 (Axitec Energy, Germany), selected based on the results of calculating the livestock complex's need for electrical power. The technical characteristics of the selected PV panel are given in Table 1.

The electric drive of the pumping station is implemented on the basis of a three-phase asynchronous motor, the technical parameters of which are given in Table 2. The motor is selected according to the hydraulic load of the water supply system of the complex.

The conversion of the direct current of the PV panel into three-phase alternating current is carried out by a PWM inverter on IGBT transistors, operating in the scalar U/f control mode. The parameters of the inverter and pulse-width control are given in Table 3.

Table 1. Technical characteristics of the AXM144-9-166-470 photovoltaic panel

Parameter	Value
Maximum power P_{max}, W	470
Voltage atP_{max} (V_{mp}), V	41,44
Current atP_{max} (Imp), A	10,87
Open circuit voltage V_{oc}, V	50,16
Short circuit current I_{sc}, A	11,48
Temperature coefficient (P_{max}), %/°C	−0,365
Temperature coefficient (V_{oc}), %/°C	−0,285
Temperature coefficient (I_{sc}), %/°C	+0,055
Maximum system voltageV_{max}, V	1000
Operating temperature range, °C	−40 to +85

Table 2. Technical characteristics of the asynchronous motor of the pumping station

Parameter	Value
Rated power, kW	7,5
Rated voltage, V	380
Rated stator current, A	16,5
Rated speed, rpm	1450
Nominal torque, N m	49,4
Number of pole pairs	2
Nominal efficiency, %	87
Power factorcos φ	0,83
Rotor moment of inertia, кг·м²	0,04
Insulation class	F

Table 3. Inverter and PWM control parameters

Parameter	Value
Inverter type	PWM IGBT
Switching frequency, kHz	5
DC link voltage V_dc, V	390–490
Output line voltage, V	380
Output frequency, Hz	50
Reference voltage V_ref, a.o.	1
PWM type	Sinusoidal
Simulation mode	Discrete
Discretization step, s	2×10^{-5}
Control method	Scalar U/f

Mathematical modeling and simulation were performed in the MATLAB/Simulink R2023b environment (MathWorks, USA). Illumination measurements for the analysis of the lighting system were carried out with a calibrated luxmeter. Two types of luminaires were studied: a luminaire with a sodium lamp ZhKU-11U-70-011 (70 W) and an LED luminaire (45 W).

Mathematical model of a photovoltaic panel

The photovoltaic panel was modeled using a single-diode equivalent circuit with series resistance R_s and parallel resistance R_p, which provides sufficient accuracy with acceptable computational complexity (Errouha et al., 2020; Selem et al., 2023). The PV-module output current is calculated using Equation 1:

$$I = I_{ph} - I_0 \cdot [\exp((V + I \cdot R_s) / / (A \cdot VT)) - 1] - (V + I \cdot R_s) / R_p \quad (1)$$

where: I is the output current, A; V is the terminal voltage, V; I_{ph} is the photocurrent, A; I_0 is the diode reverse-saturation current, A; R_s is the series resistance, Ω; R_p is the parallel resistance, Ω; A is the diode ideality factor, dimensionless; V_T = nkT/q is the thermal voltage, V; n is the number of series-connected cells, dimensionless; k = 1.381×10^{-23} J/K is the Boltzmann constant; T is the cell temperature, K; and q = 1.602×10^{-19} C is the elementary charge.

The photocurrent I_{ph} depends on solar irradiance G and cell temperature T and is determined using Equation 2:

$$I_{ph} = (I_{ph,ref} + KI \cdot \Delta T) \cdot G / G_{ref} \quad (2)$$

where: $I_{ph,ref}$ is the photocurrent under reference conditions, A; G is the solar irradiance, W/m²; G_{ref} = 1000 W/m² is the reference irradiance; T_{ref} = 25 °C is the reference cell temperature; K_I is the temperature coefficient of short-circuit current, A/°C; and $\Delta T = T - T_{ref}$ is the cell-temperature difference, °C.

The temperature dependence of the diode reverse-saturation current is described by Equation 3:

$$I_0 = I_{0,ref} \cdot (T / T_{ref})^3 \cdot \cdot \exp[q \cdot E_g / (A \cdot k) \cdot (1/T_{ref} - 1/T)] \quad (3)$$

where: E_g = 1.12 eV is the silicon band-gap energy; q = 1.602×10^{-19} C converts the electronvolt value to joules in the exponential term; $I_{0,ref}$ is the reverse-saturation current at the reference temperature, A; T and T_{ref} are the actual and reference cell temperatures, respectively, K; A is the diode ideality factor, dimensionless; and k = 1.381 × 10^{-23} J/K is the Boltzmann constant. The model parameters were obtained from the AXM144-9-166-470 data sheet under standard test conditions.

Model of an electromechanical system in MATLAB/Simulink

The electromechanical system is implemented as a complex simulation model in the MATLAB/Simulink environment (Figure 1), which reproduces the complete energy conversion chain – from the PV power source through the inverter and asynchronous electric drive to the pump load (Voznyak et al., 2021; Vydysh and Yaroshenko, n.d.).

The DC Voltage Source block represents the PV-array output. A series resistance R_s and inductance L represent the internal resistance and parasitic inductance of the input circuit, whereas the parallel resistance R_p represents the shunt branch of the single-diode equivalent circuit. The input current is measured by the Current Measurement block, and the DC-link voltage U_{dc} is exported through To Workspace blocks for subsequent processing.

The PWM IGBT Inverter block converts the DC-link voltage into three-phase AC voltage. Gate pulses are generated by the Discrete PWM Generator from the reference voltage V_{ref} and

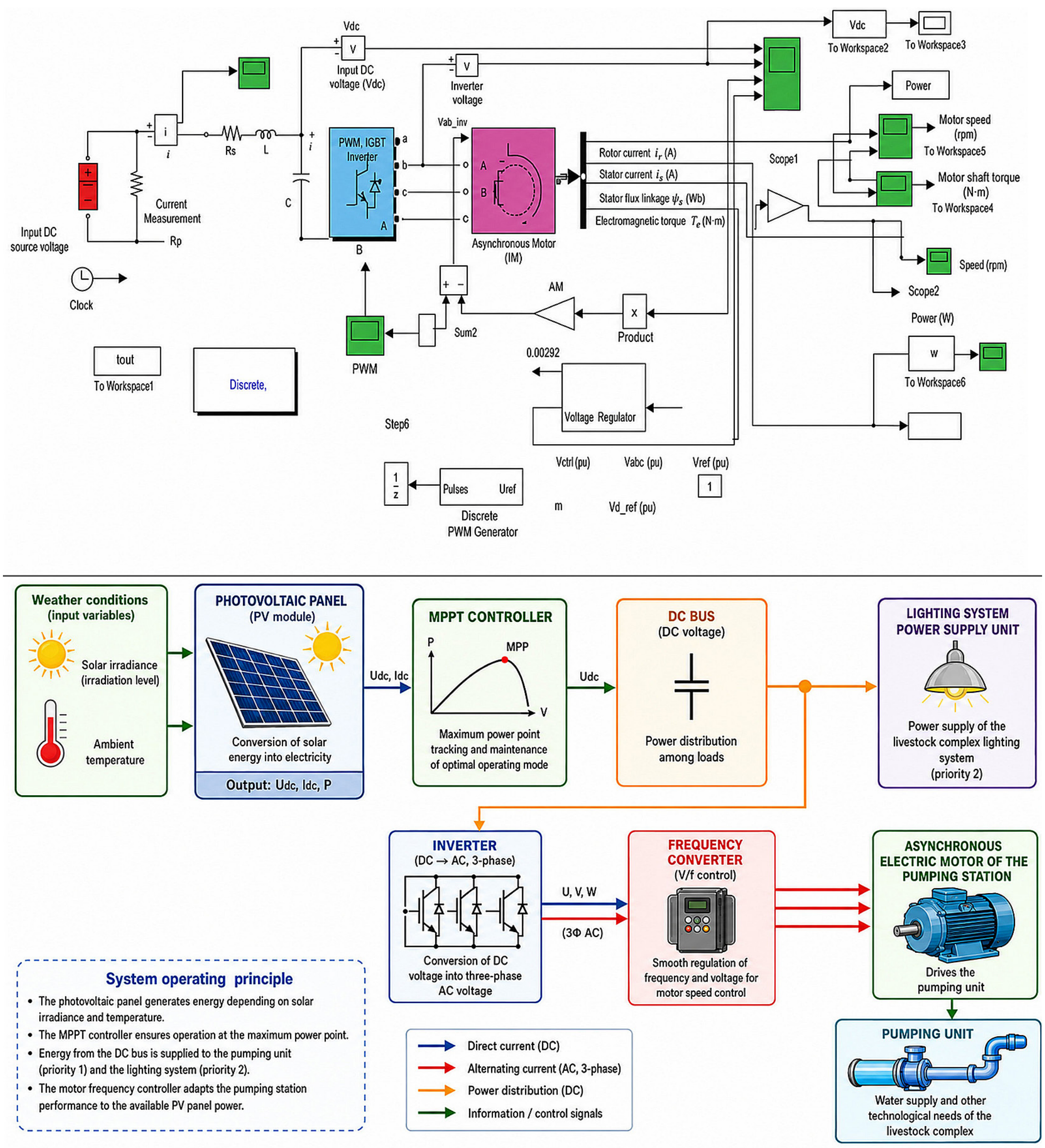

Figure 1. Simulation model of the electromechanical system of an autonomous photovoltaic station in the MATLAB/Simulink environment

normalized three-phase reference signals V_{abc}. The discrete simulation mode represents the digital control used in modern frequency converters (Voznyak and Shtuts, 2020; Stadnik et al., 2025b).

The presented model (Figure 2) reproduces the complete energy conversion chain: from the photovoltaic power source through the inverter and the asynchronous electric drive to the pump load. It is used for further analysis of transients at nominal and reduced input voltage.

The induction motor is represented by the standard Asynchronous Machine block. The monitored output signals are the phase-A rotor current $i_{r,a}$, the phase-A stator current $i_{s,a}$, the rotor angular velocity ω_m, the electromagnetic torque T_e, N·m, and the stator flux linkage φ_s, Wb. The signals are displayed by Scope blocks and exported for transient-response analysis.

The mechanical load of the pumping unit is described by the quadratic torque relation given in Equation 4:

$$T_L = T_0 + kp \cdot \omega m^2 \tag{4}$$

where: T_L is the pump-load torque, N·m; T_0 is the static-friction torque, N·m; k_p is the hydraulic load coefficient, N·m·s²/rad²; and ω_m is the rotor angular velocity, rad/s.

The Voltage Regulator generates a control signal based on feedback from the motor speed. The angular velocity is converted from rad/s to rpm by the Product block with a coefficient of 30/π. The load on the motor shaft is simulated by the Step block, which is activated at time t = 1 s.

Methodology for determining the illumination of livestock premises

The illumination levels in the production premises of the livestock complex, powered by an autonomous PV station, were estimated using the developed methodology, which is based on experimental photometric measurements and nonlinear regression modeling.

Since illuminance decreases nonlinearly with increasing distance from the light source, the experimental data were approximated using the following single-factor power-law regression model:

$$E = \beta_1 / d^{\beta_2} \tag{5}$$

where: E is the illuminance, lx; d is the distance from the luminaire, m; β_1 is the regression scale coefficient, whose units depend on the fitted exponent; and β_2 is the dimensionless exponent. The coefficients were determined from measurements at five control distances: d = 1.0, 2.0, 2.5, 5.0, and 8.0 m.

The regression coefficients were estimated from the measured illuminance values E_i at the corresponding distances d_i. Measurements were

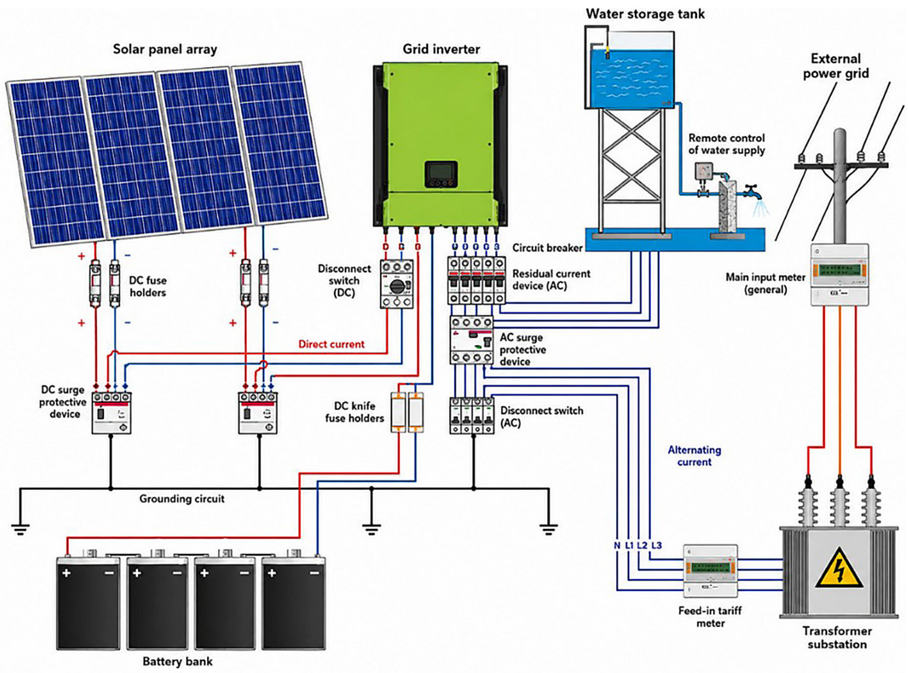

Figure 2. Scheme of the model of the studied system

performed with a calibrated luxmeter under the actual operating conditions of the lighting installation. Experimental luminous-intensity curves were constructed for each luminaire and compared with manufacturer data and calculated illuminance values.

The influence of the reflected illuminance component – estimated within 5–35 lux depending on the position of the measurement point – was taken into account by shielding the walls of the measurement room with materials with a minimum reflection coefficient (black matte fabric). The methodology was applied to two types of luminaires in order to compare their lighting and energy characteristics under conditions of autonomous photovoltaic power supply.

RESULTS

Research and development of the structural diagram of the electric drive system

The central element of the studied hybrid power supply system of the livestock complex is a photovoltaic panel – a device capable of converting solar radiation directly into electrical energy due to the photovoltaic effect. For correct modeling of this device, data on weather conditions – the level of irradiation and ambient temperature – are absolutely necessary as input variables. The output parameters of the model can be current, voltage or power of the photovoltaic panel. Any change in input values directly affects the output results, therefore, the use of an adequate and accurate mathematical model is fundamentally important (Errouha et al., 2020).

The model must necessarily reflect the influence of the level of irradiation and temperature on the parameters of the photovoltaic module, since it is these factors that determine the real output power of the system under operating conditions at the livestock complex. In this work, a model with one diode with series and parallel resistors is used, which provides sufficient accuracy with acceptable computational complexity (Kumar and Singh, 2018). The more perfect the equivalent circuit of the model, the greater the number of unknown parameters it contains. It should be noted that most of the technical passports of photovoltaic panel manufacturers do not contain comprehensive information about the parameters that depend on weather conditions – irradiation and temperature. Therefore, to build a mathematical model of a photovoltaic panel, it is necessary to make certain assumptions about the physical nature of its behavior. The main goal of the model under study is to obtain at any time the maximum power close to the real experimental values (Errouha et al., 2021).

The external characteristic of the panel I(V) is a nonlinear equation with a set of parameters that are classified as follows: those provided by the manufacturer in the technical passport; those that are known physical constants; and those that need to be calculated based on known data. In a number of simplified approaches, some unknown parameters are considered constant values. For example, in models of moderate complexity, only the series resistance R_s is taken into account without the parallel resistance, since the parallel resistance is considered large enough to be neglected (Errouha et al., 2020). In other works, both resistances are neglected simultaneously, considering the series resistance to be very small, and the parallel resistance to be very large.

However, in modern scientific literature there are works in which both internal characteristics of the photovoltaic module are considered important and are taken into account with greater accuracy (Kumar and Singh, 2018). In addition to the resistances, it is necessary to determine other key parameters: photocurrent I_{ph}, saturation current I_0 and ideality factor A. The structural diagram of the studied electric drive system includes the following main blocks: a photovoltaic panel, a maximum power point controller MPPT, an inverter, an asynchronous electric motor of the pumping station and a power supply unit for the lighting system of the livestock complex (Patel and Shah, 2025). The MPPT controller provides continuous tracking of the maximum power point on the volt-ampere characteristic of the photovoltaic panel and maintains its optimal operating mode regardless of the current weather conditions (Hontaruk et al., 2024; Errouha et al., 2021). The inverter converts the direct voltage coming from the photovoltaic panel into an alternating three-phase voltage to power the asynchronous electric motor of the pumping unit (Kaletnik et al., 2023; Voznyak et al., 2023; Vydmysh and Shtuts, 2021).

Frequency control of an asynchronous motor is a key element of the electric drive system, as it allows smooth adjustment of the rotation speed and, accordingly, the performance of the pumping station depending on the current power generated by the photovoltaic panels (Kumar and Sahu, 2022). This is especially important in conditions of variable insolation, typical of real operating conditions (Stadnik et al., 2025a). In parallel with the power supply of the pumping unit, the system provides a stable power supply for lighting the production premises of the livestock complex, which is the second priority load of the system.

The developed structural diagram of the electric drive system is a comprehensive technical solution that ensures effective conversion and distribution of solar energy between the two main consumers of the livestock complex - pumping equipment and lighting system - taking into account changing weather conditions and the needs of the production process (Stadnik et al., 2025a; Patel and Shah, 2025).

The simulation was performed for two operating modes: the nominal DC-link voltage U_{dc} = 490 V and the reduced voltage U_{dc} = 390 V, representing lower available photovoltaic power. The analysis focused on voltage, stator and rotor currents, rotational speed, electromagnetic torque, and input power (Rekioua et al., 2023; Sharma and Rawal, 2023). Based on the calculated power demand, the AXM144-9-166-470 photovoltaic panel was selected; its technical characteristics are presented in Table 1.

The model shown in Figure 2 was used for two simulation experiments at nominal and reduced DC-link voltages. At t = 1 s, a 10 N·m step change in shaft load torque was applied. The hydraulic load coefficient used in Equation 4 was determined from the nominal operating point using Equation 6:

$$k_p = T_{L,n} / \omega_n^2 = 68 / (152.6)^2 = 0.00292 \text{ N·m·s}^2/\text{rad}^2 \quad (6)$$

where: $T_{L,n}$ = 68 N·m is the nominal pump-load torque and ω_n = 152.6 rad/s is the nominal rotor angular velocity. The resulting coefficient was used in both simulation experiments.

Transients at nominal input voltage

Figure 3 presents the functional diagram of the soft-start device. The device gradually increases the voltage applied to the induction-motor windings during start-up, thereby limiting starting current and mechanical shock. This function is particularly important in an autonomous photovoltaic system with limited available source power.

The first simulation experiment was performed at the nominal DC-link voltage U_{dc} = 490 V, representing sufficient photovoltaic generation under the considered operating conditions.

The transient responses presented in Figure 4 show that the motor voltage rises smoothly to approximately 380 V. The stator and rotor currents initially increase during start-up and then approach their steady-state values. The pumping-unit motor reaches the specified speed in approximately 1.1 s, while the electromagnetic torque stabilizes after the transient interval. These results demonstrate stable start-up and steady operation at the nominal DC-link voltage.

The nominal operating condition used in the first simulation experiment is given by Equation 7:

$$U_{dc} = 490 \text{ V} \quad (7)$$

The nominal-voltage transient responses are shown in Figure 4. The results confirm the operability and dynamic stability of the electromechanical system under the nominal operating condition.

Transients when input voltage decreases

Photovoltaic systems operate under variable solar irradiance and cell temperature, which affects the available DC-link voltage and power (Errouha et al., 2020; Kumar and Singh, 2018). To evaluate this condition, the second simulation experiment reduced the DC-link voltage from 490 to 390 V while retaining the same control structure and load-change scenario.

The transient responses presented in Figures 5 and 6 show that reducing U_{dc} by 100 V decreases the available electrical power, motor currents, and electromagnetic torque. After the transient interval, the main variables stabilize at a new steady-state level, indicating that the system remains dynamically stable under the reduced-input condition (Kumar and Sahu, 2022; Patel and Shah, 2025).

The reduced-voltage experiment therefore confirms that the system can continue operating without an emergency shutdown under the specific reduced-power condition considered in this study.

The reduced operating condition used in the second simulation experiment is given by Equation 8:

$$U_{dc} = 390 \text{ V} \quad (8)$$

The corresponding transient responses are presented in Figures 5 and 6.

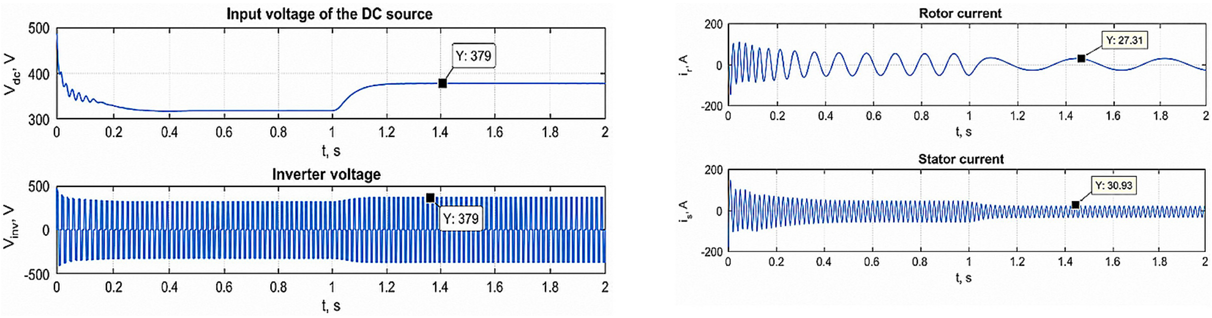

Figure 3. Motor transients at nominal input voltage Udc = 490 V

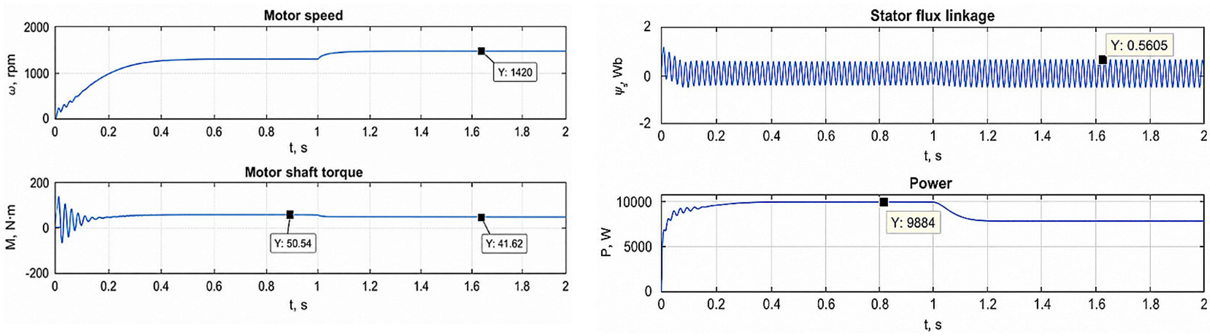

Figure 4. Motor transients at nominal input voltage

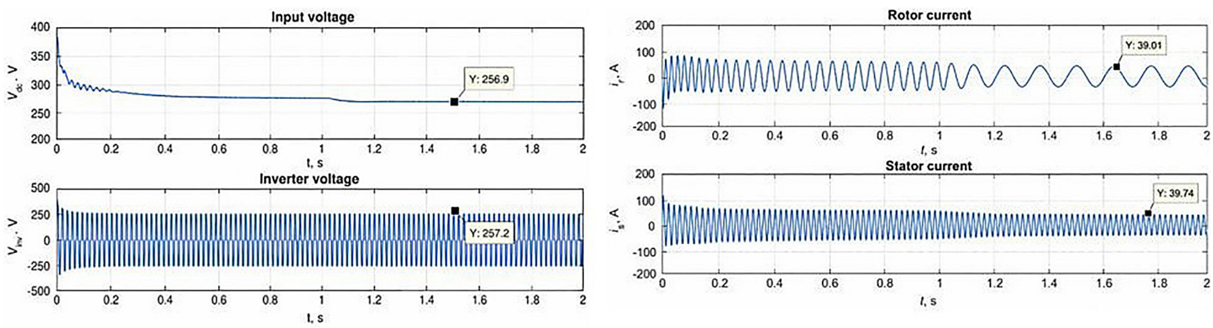

Figure 5. Motor transients at reduced input voltage Udc = 390 V

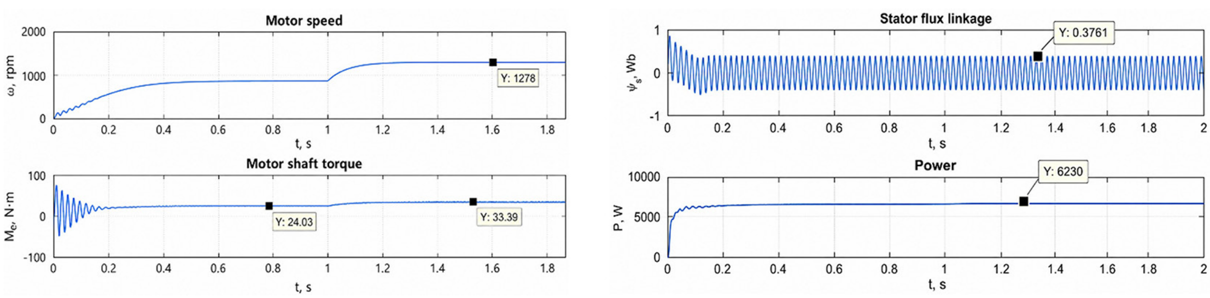

Figure 6. Motor transients at reduced input voltage

Results of a study of the illumination of livestock premises with autonomous photovoltaic power supply

As a result of the application of the developed methodology, the level of illumination of livestock premises under conditions of power supply from an autonomous photovoltaic station was estimated. The main attention was paid to the analysis of the actual values of illumination at the control points, as well as to the comparison of the lighting and energy characteristics of the lamp with a sodium lamp ZhKU-11U-70-011 with a power of 70 W and an LED lamp with a power of 45 W.

The results obtained show that the level of illumination varies depending on the distance to the light source and the type of lamp used. The nature of the change in illumination makes it possible to assess the uniformity of the light field in the room and identify areas where the illumination may be insufficient to ensure the regulatory conditions for keeping animals. This is of practical importance for choosing a rational scheme for placing lamps in livestock premises.

A comparison of the studied light sources shows that the LED lamp with a lower installed power provides more efficient use of electrical energy, which is especially important for autonomous photovoltaic systems. Reducing the energy consumption of the lighting load allows you to reduce the load on the photovoltaic station and increase the overall energy efficiency of the hybrid power supply system of the livestock complex.

The application of the proposed methodology in the conditions of autonomous photovoltaic power supply allows you to quickly assess the compliance of the actual levels of illumination with regulatory requirements, identify areas of insufficient lighting and develop measures to increase the efficiency of the lighting system of the livestock complex. This, in turn, contributes to the rational use of electrical energy generated by the photovoltaic station and increases the overall energy efficiency of the hybrid power supply system of the complex.

For comparison with the general power-law model in Equation 5, a simplified inverse-distance regression was also fitted to the measured data using Equation 9:

$$E(d) = b_0 + b_1 / d \quad (9)$$

where: $E(d)$ is the illuminance at distance d, lx; b_0 is the intercept, lx; b_1 is the inverse-distance regression coefficient, lx·m; and d is the distance from the luminaire, m. The coefficients were estimated from measurements at d = 1.0, 2.0, 2.5, 5.0, and 8.0 m.

Based on the proposed methodology, experimental measurements and mathematical modeling were performed. The comparison results are presented in Figure 7.

As a result of the application of the developed methodology, the level of illumination of livestock premises under conditions of power supply from an autonomous photovoltaic station was estimated. The main attention was paid to the comparison of the actual illumination values for a lamp with a sodium lamp ZhKU-11U-70-011 with a power of 70 W and an LED lamp with a power of 45 W.

Figure 7 compares five approaches to illuminance determination. Curve 1 was calculated from an experimentally reconstructed luminous-intensity curve based on measurements at 15 m. Curve 2 represents the nonlinear single-factor regression model. Curve 3 shows direct luxmeter measurements. Curve 4 was calculated from an experimental luminous-intensity curve obtained at 2.5 m. Curve 5 was calculated from the manufacturer's luminous-intensity data for the ZhKU-11U-70-011 sodium luminaire. At distances greater than approximately 8 m, the discrepancy between experimental and calculated values decreases because the luminaire can be approximated as a point source. At shorter distances, the curve reconstructed from measurements at 2–2.5 m better represents the actual light distribution and is more suitable for practical energy audits of livestock premises.

Curve 5, based on the manufacturer's tabular data, is similar in shape to the experimentally obtained one, but is located somewhat lower. The main reason for this discrepancy is the presence of a reflected component of illumination in the research room, which leads to an overestimation of the luxmeter readings. Approximate measurements showed that the value of the reflected component varies within 5–35 lux, on average about 20 lux depending on the position of the measurement point, which is consistent with the difference between curves 3 and 5. Analysis of graphical dependencies shows that in real energy audit conditions, more reliable results are achieved when using a light intensity curve constructed on the basis of close-up measurements

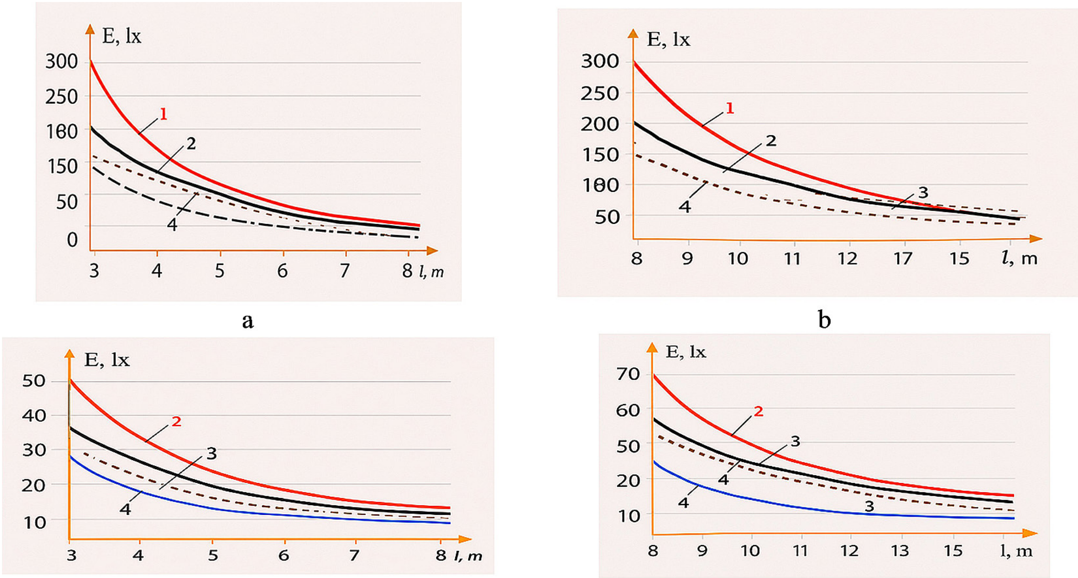

Figure 7. Results of research on a luminaire with a sodium lamp (a, b) and with LEDs (c, d)

at a distance of about 2.5 m. An additional advantage is the ability to perform measurements manually without special lifting equipment. To increase the reliability of the results, it is necessary to minimize the influence of the reflected component of illumination by shielding the walls with materials with a minimum reflection coefficient, for example, black matte fabric. Building a regression model can be used to cross-check the results obtained. The analysis shows that for LED lamps the nature of the dependencies is similar, which confirms the universality of the proposed method and the feasibility of its application in optimizing artificial lighting systems for livestock premises with autonomous photovoltaic power supply.

Figure 8 shows the luminous intensity curves of the studied luminaires, constructed using the method proposed above.

Figure 9 shows the ground-level illuminance produced by a luminaire mounted at a height of 8 m. The calculation uses luminous-intensity curves in the transverse meridian plane. Analysis of Figure 9 shows that the LED luminaire provides at least 4 lx up to a distance of approximately 10 m, whereas the sodium luminaire reaches approximately 13 m. The difference reflects the distinct light-distribution characteristics of the two luminaires.

From the standpoint of energy audit, it is advisable to use an LED luminaire, which, while providing the regulatory level of illumination, is characterized by significantly lower energy consumption. The power of an LED luminaire is 45 W, which is approximately 35% less compared to the power of a luminaire with a sodium lamp. This allows us to significantly reduce electrical energy consumption and operating costs, which is especially important in the context of optimizing artificial lighting systems for livestock premises.

An additional recommendation of the energy auditor in this case may be the feasibility of improving the light distribution characteristics of the LED luminaire. In particular, expanding the transverse light intensity curve by using special optical lenses or secondary optics would allow increasing the area of effective lighting without increasing the installed power. Such an approach would contribute to increasing the uniformity of lighting and further increasing the energy efficiency of the lighting installation, which meets modern energy saving requirements and the results of the energy audit.

Experimental studies conducted for luminaires with sodium lamps and LED sources confirmed the possibility of restoring light distribution characteristics based on the results of measurements with a luxmeter. It was established that the accuracy of the approximate determination of illumination significantly depends on the measurement distance: at longer distances (over ~8 m) the luminaire can be considered with sufficient accuracy as a point source, while at shorter distances it is necessary

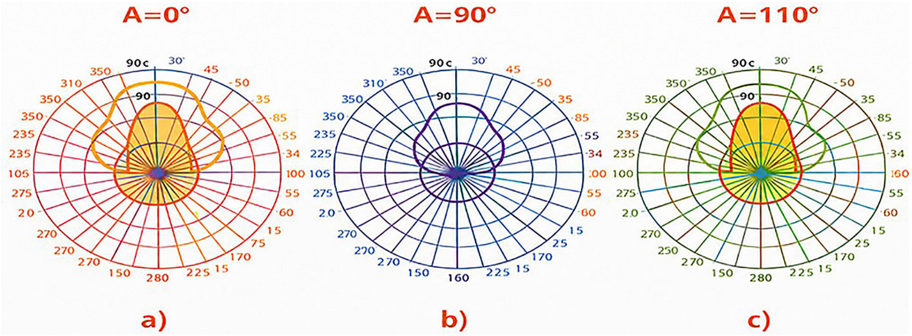

Figure 8. Luminous intensity curves for luminaires with LEDs (1) and with a sodium lamp (2) in the meridian planes 0º (a), 45º (b), 90º (c)

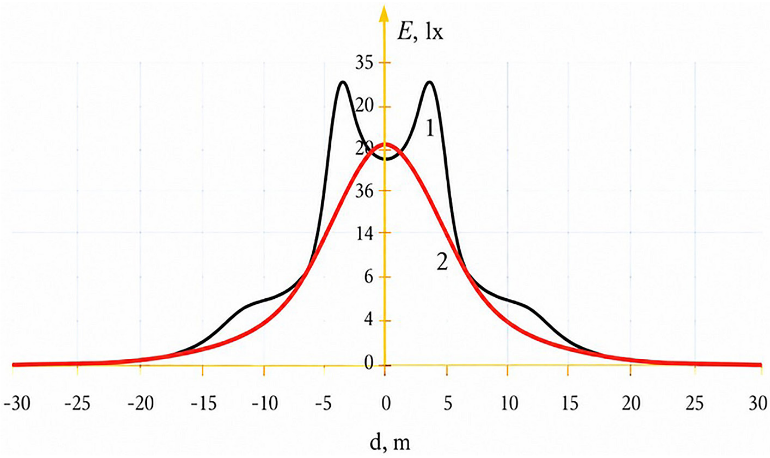

Figure 9. Calculation of illumination at a distance d from a lighting pole, 8 m high: 1 – for a luminaire with a sodium lamp, 2 – for a luminaire with LEDs

to take into account the influence of geometry and real light distribution.

The proposed method combines an experimentally reconstructed luminous-intensity curve with regression modeling of illuminance as a function of distance. The regression approach provides a useful cross-check, whereas measurements at 2–2.5 m offer a practical method for energy-audit applications within distances up to approximately 8 m, provided that the reflected illuminance component is considered.

A comparative analysis has shown that an LED luminaire, provided that the regulatory illuminance is provided, has an advantage in terms of energy consumption, although it may be inferior in terms of the effective lighting range due to the peculiarities of light distribution. It is substantiated that within the framework of an energy audit it is advisable not only to assess the compliance of illuminance with standards, but also to formulate recommendations for increasing energy efficiency and improving light distribution (in particular, the use of secondary optics) without increasing the installed power.

Development of technical and technological support for the electromechanical system of an autonomous photovoltaic station

The technical and technological support of the studied hybrid power supply system of the livestock complex is implemented on the basis of a simulation model developed in the MATLAB/Simulink environment. The model reproduces the main stages of energy conversion: generation of electric energy by a photovoltaic source, its conversion by an inverter, powering the asynchronous electric drive of the pumping station and forming a mechanical load on the motor shaft.

The developed model was used as a tool to check the coordinated operation of the main elements of the system – the photovoltaic source, the inverter, the asynchronous electric drive and the pump load. This made it possible to assess the performance of the electromechanical system under different power supply modes, in particular at the nominal input voltage of the photovoltaic panel and when it decreases due to changes in solar insolation conditions.

This approach allows not only to verify the correctness of the technical decisions made, but also to analyze the dynamic characteristics of the system: changes in voltage, stator and rotor currents, motor rotation speed and electromagnetic torque. The results obtained are the basis for further assessment of the stability and efficiency of the autonomous photovoltaic station as part of the hybrid power supply of the livestock complex.

The conversion of electrical energy from the photovoltaic source to the asynchronous electric drive was carried out through an inverter converter with pulse-width control. The parameters of the inverter and PWM control given in the research methodology were taken into account during the modeling of transient processes, which made it possible to evaluate the operation of the pump electric drive at nominal and reduced power levels.

In the modeling process, the asynchronous electric drive of the pumping station was considered as the main executive element of the electromechanical system (Figure 10). Analysis of its output parameters made it possible to evaluate the change in stator and rotor currents, angular velocity, electromagnetic torque and the stability of the system at different levels of the input voltage of the photovoltaic panel.

The control system generated the control action from motor-speed feedback and reproduced the shaft-load change of the pumping unit. This made it possible to evaluate stabilization of the main variables after changes in the power-supply condition (Stadnik et al., 2025d).

A comparative analysis of the two studied operating modes of the system, the results of which are summarized in Table 4, confirms that a decrease in the input voltage of the photovoltaic panel by 100 V leads to a proportional decrease in the energy performance of the system. At the same time, the system remains stable and does not require an emergency shutdown, which is a critically important characteristic for the continuous provision of water supply and lighting of the livestock complex.

Table 4. Comparative analysis of system operating modes at different input voltage values

Parameter	Nominal mode Udc = 490 V	Reduced mode Udc = 390 V	Deviation, %
Input voltage, V	490	390	−20,4
Engine voltage, V	380	~302	−20,5
Stator current, A	16,5	~13,1	−20,6
Shaft torque, N m	49,4	~31,2	−36,8
Time to reach the set speed, s	1,1	1,4	+27,3
Power consumption, kW	7,5	~4,7	−37,3
System stability	Stable	Stable	–
Emergency shutdown	Missing	Missing	–

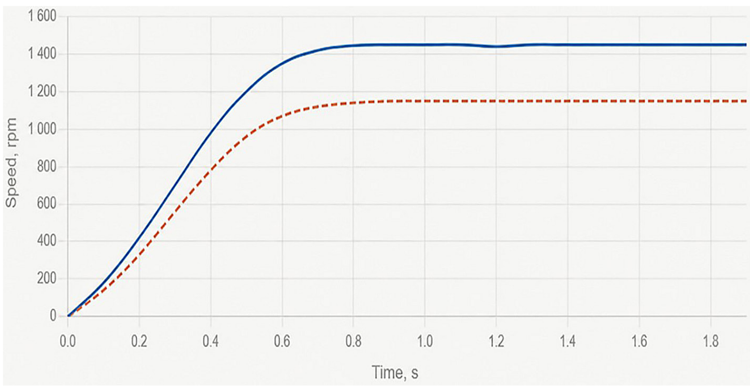

Figure 10. Transient process of the rotation speed of the asynchronous motor of the pumping station at the nominal (Udc = 490 V) and reduced (Udc = 390 V) input voltage of the photovoltaic module

Environmental justification of the system

The environmental assessment compares the proposed photovoltaic system with a diesel-generator scenario in terms of greenhouse-gas emissions, resource use, life-cycle impacts, and qualitative circular-economy criteria.

Replacing local diesel generation with photovoltaic electricity eliminates direct emissions of CO_2, NO_x, and particulate matter at the point of use. Life-cycle emissions associated with manufacturing, transport, maintenance, replacement, and end-of-life treatment remain and are considered separately in the simplified assessment (Abbasi and Mohammadi, 2024; Errouha et al., 2020).

The environmental analysis includes: (1) a comparison of greenhouse-gas emissions for diesel and photovoltaic electricity; (2) a screening assessment of life-cycle greenhouse-gas impacts; (3) an evaluation of circular-economy criteria; and (4) a qualitative mapping of the technical and environmental results to relevant UN Sustainable Development Goals.

Comparative analysis of greenhouse gas emissions

For the diesel-generator scenario, direct CO_2 emissions were calculated using a fuel-consumption factor of 0.30 L/kWh and a diesel-combustion emission factor of 2.65 kg CO_2/L. For the functional unit of 66 kWh/day, diesel consumption is 19.8 L/day and direct emissions are 52.47 kg CO_2/day (Abbasi and Mohammadi, 2024).

For the photovoltaic scenario, a harmonized life-cycle greenhouse-gas intensity of 46 g CO_2-eq./kWh was adopted from the reported range of 41–50 g CO_2-eq./kWh for monocrystalline silicon PV systems (Errouha et al., 2020; Kumar and Singh, 2018). For 66 kWh/day, this corresponds to 3.04 kg CO_2-eq./day.

The daily electrical-energy yield of one photovoltaic panel was estimated using equivalent peak-sun hours for the Vinnytsia region. The daily energy yield is calculated using Equation 10:

$$E_{day} = P_{rated} \times \eta_{sys} \times t_{PSH} = \\ = 0.470 \times 0.85 \times 4.5 \approx 1.80 \text{ kWh/day} \quad (10)$$

where: E_{day} is the daily electrical-energy yield per panel, kWh/day; P_{rated} = 0.470 kW is the rated panel power; η_{sys} = 0.85 is the overall system efficiency, accounting for inverter, wiring, and MPPT-controller losses; and t_{PSH} = 4.5 h/day is the adopted equivalent peak-sun duration.

The functional electricity demand is 66 kWh/day, comprising approximately 60 kWh/day for pumping and 6 kWh/day for lighting.

The minimum number of panels based on daily energy balance is determined using Equation 11:

$$N_{\text{panel}} = W_{\text{gen}} / W_{\text{day}} = 66 / 1.8 \approx \\ \approx 37 \text{ N= } 66 / 1.8 \approx 37 \text{ panels} \quad (11)$$

A comparative analysis of the environmental performance of the diesel and photovoltaic scenarios is presented in Table 5. The array design must additionally satisfy the inverter DC-voltage range and the required instantaneous motor power; therefore, the final series-parallel configuration should be specified during detailed system design.

As shown in Table 5, the photovoltaic scenario reduces greenhouse-gas emissions from

Table 5. Functional blocks of the MATLAB/Simulink model and their purpose

Model block	Type	Function in the system
DC Voltage Source	Source	Photovoltaic panel output voltage simulation
Rs, L	Passive elements	Internal resistance and inductance of a circuit
Rp	Passive element	Parallel resistance of the photocell model
Current Measurement	Measurement	Input current measurement
PWM IGBT Inverter	Transformer	Inverting DC voltage to three-phase AC
Discrete PWM Generator	Management	PWM pulse generation for the inverter
Asynchronous Machine	Engine	Model of asynchronous motor of the pumping unit
Voltage Regulator	Regulator	Voltage feedback control
Product + 30/π	Transformation	Convert rad/s to rpm
Step6	Task	Putting load on the motor shaft
Clock + To Workspace	Record	Fixing the timeline and modeling results
Scope1, Scope2	Visualization	Real-time transient display

approximately 52.47 kg CO_2/day to 3.04 kg CO_2-eq./day, corresponding to a reduction of about 94.2%. The annual reduction is approximately 18.04 t CO_2-eq., and avoided diesel consumption is approximately 7.227 L/year. The photovoltaic configuration also substantially reduces the operational risk of soil and groundwater contamination associated with diesel storage and accidental fuel spills.

Compliance with the principles of the circular economy

The circular economy promotes reduced use of primary resources, longer product life, repair and reuse, material recovery, and waste prevention. The studied system was evaluated qualitatively against these criteria (Koval et al., 2025a, 2025b).

The concept of the Circular Economy envisages a closed cycle of resource use: waste minimization, maximum reuse of materials, and the transition from a linear model of "extraction – production – disposal" to a circular one (Koval et al., 2025a). The studied photovoltaic system meets the key principles of the circular economy according to the following criteria:

- Using an inexhaustible natural resource – solar radiation – as the main source of energy, which completely eliminates the consumption of exhaustible fossil fuels during operation.
- The long service life of PV panels – 25–30 years – significantly exceeds the similar indicator of diesel generators (10–15 years), which reduces the frequency of equipment replacement and the volume of waste.
- The major material fractions of modern PV modules, including glass, aluminum, silicon, and copper, are technically recoverable; however, actual recovery rates depend on available collection and recycling infrastructure and should not be assumed to equal a fixed percentage in all regions.
- Using LED lighting (45 W) instead of sodium lamps (70 W) reduces electricity consumption by the lighting system by 35%, which increases the life of batteries and reduces the number of charge-discharge cycles.
- Compared with a diesel-generator scenario, the photovoltaic system substantially reduces the routine use of liquid fuel and lubricants and therefore lowers, but does not completely eliminate, the risk of chemical contamination of soil and water during operation.

Thus, the proposed system is consistent with key circular-economy objectives through reduced fossil-fuel consumption, long equipment service life, recoverable material fractions, and lower operational waste generation.

Life cycle assessment

Life cycle assessment (LCA) is governed by ISO 14040:2006 and ISO 14044:2006. In this study, a simplified screening-level comparative assessment was performed in Microsoft Excel 365 for two electricity-supply scenarios: a diesel generator and an autonomous photovoltaic station (Figure 11). The functional unit was the delivery of 66 kWh/day to pumping and lighting loads over 25 years. The cradle-to-grave boundary included equipment production, transport, installation, operation, maintenance, diesel consumption, and end-of-life treatment. No commercial process

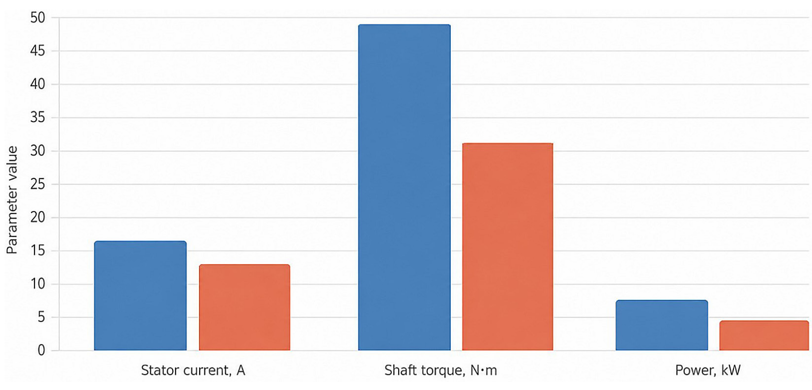

Figure 11. Comparative diagram of the main parameters of the electromechanical system in different operating modes of the photovoltaic station

database such as ecoinvent or GaBi was used; instead, diesel-emission factors from the cited literature and harmonized PV life-cycle greenhouse-gas values reported by NREL-related and peer-reviewed sources were applied. The indicator was global-warming potential expressed in kilograms of CO_2-equivalent. Because detailed primary inventory data for batteries, inverters, transport distances, and component-replacement schedules were unavailable, the results should be interpreted as a screening comparison rather than a full product-specific LCA.

The screening results presented in Table 6 indicate approximately 478,800 kg CO_2 for the diesel scenario and 27,700 kg CO_2-eq. for the photovoltaic scenario over 25 years, assuming constant delivery of 66 kWh/day. The photovoltaic result is therefore approximately 17 times lower. The reported ecological payback range of 1.5–2.5 years is retained as a literature-based estimate for monocrystalline PV systems and may vary with manufacturing electricity mix, solar resource, and system configuration (Errouha et al., 2020; Kumar and Singh, 2018).

Compliance with the UN sustainable development goals (SDGs)

The studied hybrid photovoltaic power supply system for the livestock complex directly supports the implementation of seven of the seventeen UN sustainable development goals (SDGs) adopted within the framework of the 2030 Agenda (Table 7).

The SDG assessment is based on a transparent indicator-to-target mapping: reliable water pumping supports SDG 6; renewable electricity and energy efficiency support SDG 7; reduced operating costs and resilient agricultural production support SDG 8; deployment of intelligent energy infrastructure supports SDG 9; material recyclability and reduced fuel use support SDG 12; quantified greenhouse-gas reductions support SDG 13; and reduced risk of soil and groundwater contamination supports SDG 15.

The contribution to SDG 13 is associated with the quantified reduction in greenhouse-gas emissions, while the broader mapping to SDGs 6, 7, 8, 9, 12, and 15 reflects improved water-supply reliability, renewable-energy use, resilient agricultural infrastructure, resource efficiency, and reduced pollution risk. This mapping is qualitative and does not constitute formal certification of SDG compliance.

Table 6. Comparative analysis of CO_2 emissions and environmental performance of power supply systems of the livestock complex

Parameter	Diesel generator	PV station(AXM144-9-166-470)	Saving
Specific CO_2 emissions, g/kWh	820	~46 (LCA)	≈ 94,4%
Fuel consumption, l/h	~1,8–2,2	0	100%
Daily production, kWh/day	~60	~60	–
CO_2 emissions per day, kg/day	~49,2	~2,76	~46,4 kg/day
CO_2 emissions per year, t/year	~17,95	~1,01	~16,94t/year
Noise during operation, dB	75–95	0 (quiet)	–
Risk of fuel spillage	Present	Missing	–
Need for maintenance	Monthly	1 time per year	–

Table 7. Comparative LCA assessment of a diesel generator and a PV station (functional unit: 66 kWh/day, 25 years)

Life cycle stage	Diesel generator	FE panel AXM144-9-166-470
Equipment manufacturing	~500 kg CO_2-eq./kW	~1500 kg CO_2-eq./kW
Transportation	Fuel + logistics	One-time
Operation (25 years)	820 g CO_2/kWh × 25 years.	~0 g CO_2/kWh
Cumulative emissions over 25 years	~450,000 kg CO_2-eq.	~26,000 kg CO_2-eq.
Utilization	Scrap metal + waste oil	95% of components are recyclable
Service life	10–15 years	25–30 years old

Table 8. Compliance of the studied system with the UN sustainable development goals

UN Sustainable Development Goal	Connection with the system under study
SDG 2: End hunger	Reliable water supply increases livestock productivity and food security
SDG 6: Clean water and sanitation	Autonomous pumped water supply without dependence on networks
SDG 7: Affordable and Clean Energy	PV station provides renewable energy for rural areas
SDG 9: Innovation and infrastructure	Implementation of MPPT and frequency control - modern technical solutions
SDG 12: Responsible consumption	Using LED lighting, reducing energy loss by 35%
SDG 13: Combating climate change	Reduction of CO_2 emissions up to 16.94 t/year compared to a diesel generator
SDG 15: Conserving ecosystems	No emissions and fuel spills - protection of soils and water bodies

Impact on the noise and electromagnetic environment. Diesel generators are recognized sources of operational noise and local exhaust emissions. In contrast, PV modules and MPPT controllers have no rotating parts. Acoustic emissions from the inverter, cooling system, and pumping equipment were not measured in this study and should be evaluated experimentally before quantitative noise-reduction claims are made (Table 8).

The inverter switching frequency was 5 kHz in the simulation model; however, switching frequency alone does not determine the audible sound-pressure level or its biological effect. These effects depend on inverter topology, enclosure, cooling, installation, and the frequency response of the surrounding equipment.

Electromagnetic compatibility was not experimentally tested in this study. The inverter and installation should therefore be selected, shielded, grounded, and verified in accordance with the applicable electromagnetic-emission and immunity standards, including EN 61000-6-4 where relevant.

Summary of the environmental justification

The environmental assessment indicates that the photovoltaic scenario has a substantially lower greenhouse-gas impact than the diesel-generator scenario under the adopted assumptions. In particular:

- Greenhouse-gas emissions decrease from approximately 52.47 kg CO_2/day to 3.04 kg CO_2-eq./day, corresponding to a reduction of about 94.2%.
- Over 25 years, the screening estimate decreases from approximately 478,800 kg CO_2 to 27,700 kg CO_2-eq., or by a factor of approximately 17.
- Routine diesel storage and fuel handling are avoided, substantially reducing the operational risk of soil and groundwater contamination from fuel spills.
- The PV array and MPPT controller contain no rotating parts; quantitative acoustic performance of the complete installation requires experimental verification.
- Reduction of electricity consumption by the lighting system by 35% due to the use of LED lamps instead of sodium lamps.
- The system supports circular-economy objectives through reduced fossil-fuel use, long service life, and recoverable material fractions, although actual recycling rates depend on regional infrastructure.
- The technical and environmental outcomes are qualitatively related to seven UN Sustainable Development Goals; this mapping is not a formal certification of compliance.

CONCLUSIONS

The work conducted a comprehensive study of the electromechanical system of an autonomous photovoltaic station for hybrid power supply of pumping equipment and lighting of livestock complexes. Based on theoretical analysis, mathematical modeling in the MATLAB/Simulink environment and experimental measurements, the following main results were obtained.

The studied system comprises an AXM144-9-166-470 photovoltaic module, an MPPT controller, a PWM inverter with a 5 kHz switching frequency, a 7.5 kW induction-motor pumping drive, energy storage, and an LED lighting subsystem. The simulations demonstrate that combining MPPT control with scalar U/f motor control provides stable operation under the nominal and reduced-input conditions considered in this study; no claim of universal optimality is made.

1. A mathematical model of the photovoltaic module and electromechanical system was developed. The PV module was represented by a single-diode equivalent circuit with series resistance R_s and parallel resistance R_p. The MATLAB/Simulink model reproduces the energy-conversion chain from the DC source through the inverter and induction motor to the pump load. The pump load is described by $T_L = T_0 + k_p\omega_m^2$.
2. At the nominal DC-link voltage U_{dc} = 490 V, the drive started stably and reached the specified speed in approximately 1.1 s. The motor voltage approached 380 V, and the currents and electromagnetic torque stabilized after the transient interval.
3. At the reduced DC-link voltage U_{dc} = 390 V, the motor voltage, current, torque, and power decreased, while the speed-settling time increased to approximately 1.4 s. The system nevertheless reached a new steady state without an emergency shutdown under the specific reduced-power condition evaluated.
4. The illumination methodology combines luxmeter measurements, experimentally reconstructed luminous-intensity curves, and nonlinear regression. Measurements at 2–2.5 m provided a practical basis for estimating illuminance at distances up to approximately 8 m, while the reflected component of 5–35 lx required consideration.
5. The 45 W LED luminaire used approximately 35% less installed power than the 70 W sodium luminaire. The LED luminaire provided at least 4 lx to approximately 10 m, whereas the sodium luminaire reached approximately 13 m because of its different light distribution. Secondary optics may improve the LED luminaire's effective coverage without increasing installed power.
6. For the functional unit of 66 kWh/day, the simplified environmental assessment estimated 52.47 kg CO_2/day for diesel generation and 3.04 kg CO_2-eq./day for photovoltaic electricity, a reduction of approximately 94.2%. Over 25 years, the screening estimates were approximately 478,800 and 27,700 kg CO_2-eq., respectively. These results are subject to the stated assumptions and should be interpreted as a screening comparison rather than a full product-specific LCA.

REFERENCES

1. Stadnik, M., Shtuts, A., Yaropud, V., Kupchuk, I. (2025a). Development of an algorithm for power supply to a livestock farm using biogas. *Energy Policy Journal, 28*(4), 1–26. https://doi.org/10.33223/epj/208465
2. Burlaka, S., Kupchuk, I., Boretska, T., Gontaruk, Y., Melnyk, M. (2024). Optimizing the process of mixing diesel fuel and biofuel in a blade mixer to improve mixture quality. *Polityka Energetyczna, 27*(3), 31–52. https://doi.org/10.33223/epj/189437
3. Kaletnik, H., Yaropud, V., Kupchuk, I., Aliiev, E., Babyn, I., Lavreniuk, P. (2023). Modeling of the technological process of walnut drying in a convective dryer. *Przeglad Elektrotechniczny, 99*(12), 91–97. https://doi.org/10.15199/48.2023.12.17
4. Aliiev, E., Malehin, R., Aliieva, O., Yaropud, V., Kukharets, S., Pidlisnyj, V., Horetska, I., Kielbasa, P., Hutsol, T. (2026). Development of a homogenizer-disperser of liquid fodder for pigs. *Scientific Reports, 16*(1), 14127. https://doi.org/10.1038/s41598-026-44547-9
5. Voznyak, O., Polievoda, Y., Kupchuk, I., Trukhanska, O., Shvets, L., Zamrii, M. (2023). Development of object detection algorithm in halftone images. *Przeglad Elektrotechniczny, 99*(11), 192–195. https://doi.org/10.15199/48.2023.11.33
6. Stadnik, M. I., Shtuts, A. A., Lypnytskyi, R. M., Kogut, V. M. (2025b). Mechatronic drive of a scraper conveyor as an integrated module of power engineering, automated and information-control systems. *Technika, Energetika, Transport APC, 4*(131), 130–139. https://doi.org/10.37128/2520-6168-2025-4-17
7. Stadnik, M., Shtuts, A., Kolisnyk, M., Hryhorenko, N. (2025c). Research on the implementation of intelligent systems to increase the reliability and efficiency of the operation of electric power complexes. *Technology, Energy, Transport of Agricultural Industry, 1*(128), 122–134. https://doi.org/10.37128/2520-6168-2025-1-14
8. Hontaruk, Y., Furman, I., Bondarenko, V., Riabchyk, A., Nepochatenko, O. (2024). Production of biogas and digestate at sugar factories as a way of ensuring the energy and food security of Ukraine. *Polityka Energetyczna, 27*(2), 195–210. https://doi.org/10.33223/epj/185210
9. Errouha, M., Derouich, A., El Ouanjli, N., Motahhir, S. (2020). High-performance standalone photovoltaic water pumping system using induction motor. *International Journal of Photoenergy*, 2020, 1–13. https://doi.org/10.1155/2020/3872529
10. Kumar, R., Sahu, S. (2022). Design and processor in the loop implementation of an improved control for IM driven solar PV fed water pumping system. *PMC.* https://pmc.ncbi.nlm.nih.gov/articles/PMC8933576/

11. Errouha, M., Motahhir, S., Combe, Q. (2021). Optimization for a photovoltaic pumping system using indirect field oriented control of induction motor. *Electronics, 10*(24), 3076. https://doi.org/10.3390/electronics10243076
12. Kumar, S., Singh, B. (2018). Standalone photovoltaic water pumping system using induction motor drive with reduced sensors. *IEEE Transactions on Industry Applications, 54*(4), 3645–3655. https://doi.org/10.1109/TIA.2018.2825285
13. Koval, V., Atstaja, D., Filipishyna, L., Udovychenko, V., Kryshtal, H., Gontaruk, Y. (2025a). Sustainability assessment and resource utilization of agro-processing waste in biogas energy production. *Climate, 13*(5), 99. https://doi.org/10.3390/cli13050099
14. Koval, V., Perović, N., Rasovic, I., Božović, D., Gontaruk, Y. (2025b). Biofuel production assessment of crop rotation systems and organic residues in agricultural management. *Agriculture, 15*(22), 2316. https://doi.org/10.3390/agriculture15222316
15. Hontaruk, Y., Bondarenko, V., Sokoliuk, K., Basyuk, D., Amirov, R. (2026). Analysis of the state, potential and marketing support of bioenergy development in Ukraine in the context of European and world experience. *Energy Policy Journal, 29*(1), 69–88. https://doi.org/10.33223/epj/205055
16. Abbasi, A., Mohammadi, A. (2024). MIWO based MPPT of PV system for induction motor driven water pumping system. *Renewable Energy Focus*. https://doi.org/10.1016/j.ref.2024.100571
17. Selem, S. I., El-Hameed, M. A., El-Fergany, A. A. (2023). Optimal performance of photovoltaic-powered water pumping system. *Mathematics, 11*(3), 731. https://doi.org/10.3390/math11030731
18. Patel, H., Shah, V. (2025). Single phase induction motor driver for water pumping powered by photovoltaic system. *Electronics, 14*(6), 1189. https://doi.org/10.3390/electronics14061189
19. Rekioua, D., Zaouche, F., Mokrani, Z., Rekioua, T. (2023). Power management control for photovoltaic water pumping system in agriculture. *Turkish Journal of Electromechanics and Energy, 8*, 109–117.
20. Augustyn, G., Mikulik, J., Rumin, R., Szyba, M. (2021). Energy self-sufficient livestock farm as the example of agricultural hybrid off-grid system. *Energies, 14*(21), 7041. https://doi.org/10.3390/en14217041
21. Sharma, K., Rawal, M. (2023). Technical modelling of solar photovoltaic water pumping system and evaluation of system performance and their socio-economic impact. *Heliyon, 9*(5), e15972. https://doi.org/10.1016/j.heliyon.2023.e15972
22. Stadnik, M. I., Shtuts, A. A., Kolisnyk, M. A. (2025d). Theoretical foundations of automation. Theory and practice. VNAU.
23. Voznyak, O. M., Shtuts, A. A., Kolisnyk, M. A. (2021). Modern electric drive systems. *Theory and practice. Part 1. TVORY.*
24. Voznyak, O. M., Shtuts, A. A. (2020). Calculation of non-standard W-parameters of a four-terminal circuit on a bipolar transistor. *Technology, Energy, Transport, 2*(109), 122–128.
25. Vydmysh, A. A., Shtuts, A. A. (2021). Research of dynamic characteristics of a closed electric drive system of a gravity concrete mixer by computer modeling. *Bulletin of KhNU. Series: Technical Sciences, 1*(293), 113–125.
26. Vydysh, A. A., Yaroshenko, L. V. (n.d.). Fundamentals of electric drive. Theory and practice. Part 1.